Solar Cells

DOI: 10.1002/anie.201203330

A Supramolecular Complex in Small-Molecule Solar Cells based on Contorted Aromatic Molecules**

*Seok Ju Kang, Jong Bok Kim, Chien-Yang Chiu, Seokhoon Ahn, Theanne Schiros, Stephanie S. Lee, Kevin G. Yager, Michael F. Toney, Yueh-Lin Loo, and Colin Nuckolls**

We recently described a supramolecular complex that forms in co-crystalline solids between doubly concave aromatic molecules and fullerenes.[1–3] Supramolecular complexes of fullerenes and aromatic compounds have been known for almost as long as fullerenes themselves.[4–6] Both hexabenzocoronenes (HBCs)[1] and dibenzotetrathienocoronenes (DBTTC)[2] form co-crystals with C_{60} or C_{70} fullerenes. In these co-crystals, the concave faces of the aromatic molecule associate with the fullerene to form a nested structure, in which the fullerene is surrounded by the electron-rich aromatic compound. When these materials are deposited as either bilayered or reticulated structures, they form efficient active layers in photovoltaic devices.[1,3] In earlier studies, we found that the fullerene and the coronene derivatives are both crystalline, with co-crystals forming at the interface between these two materials. This co-crystalline region is responsible for enhanced device performance. We studied, for the first time, the solution-based self-assembly of these contorted aromatic molecules with soluble fullerene derivatives. We hypothesized and tested, whether the self-assembly from solution can create the active layer in solar cells. We found that there is self-organization between the two organic semiconductors shown in Figure 1, the hexylated DBTTC (6-DBTTC) and phenyl-C_{70}-butyric acid methyl ester ($PC_{70}BM$). These self-assembled films are active in photovoltaic devices and provide high open circuit voltages (V_{OC}) and power conversion efficiencies (PCE) up to 2.7%. The optimal conditions to form these self-assembled heterojunctions are very different from those of polymeric photovoltaic devices.[7–10]

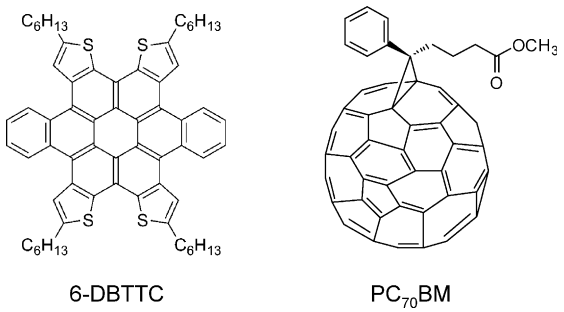

Figure 1. Chemical structure of 6-DBTTC and $PC_{70}BM$.

To test for assembly between 6-DBTTC and $PC_{70}BM$, we mixed both compounds in varying ratios and monitored the photoluminescence emission from 6-DBTTC. We found a significant amount of fluorescence quenching (see Figure S1a in the Supporting Information). From this data we could perform a Stern–Volmer analysis,[11] and it showed a significant amount of association between the two components and an association constant of $10^5\,M^{-1}$ (Figure S1b) in *o*-xylene as solvent. We speculated that the mode of association has the concave face of 6-DBTTC in contact with the convex face of the $PC_{70}BM$. This mode is similar to the organization of unsubstituted fullerenes with the contorted aromatic compounds in the solid state.[1,2]

We tested how this supramolecular complex impacts the properties of films in photovoltaic devices. We varied the ratio

[*] Dr. S. J. Kang,[+] C.-Y. Chiu, Dr. S. Ahn, Prof. C. Nuckolls
Department of Chemistry, Columbia University
New York, NY 10027 (USA)
E-mail: cn37@columbia.edu
Homepage: http://nuckolls.chem.columbia.edu/
Dr. J. B. Kim,[+] S. S. Lee, Prof. Y.-L. Loo
Department of Chemical and Biological Engineering
Princeton University
Princeton, NJ 08544 (USA)
Dr. T. Schiros
Columbia Energy Frontier Research Center (EFRC)
Columbia University
New York, NY 10027 (USA)
Dr. K. G. Yager
Center for Functional Nanomaterials
Brookhaven National Laboratory
Upton, NY 11973 (USA)
Dr. M. F. Toney
Stanford Synchrotron Radiation Lightsource
SLAC National Accelerator Laboratory
Menlo Park, CA 94025 (USA)
[+] These authors contributed equally to this work.

[**] This research was supported as part of the Center for Re-Defining Photovoltaic Efficiency Through Molecular-Scale Control, an Energy Frontier Research Center funded by the U.S. Department of Energy (DOE), Office of Science, Office of Basic Energy Sciences under award number DE-SC0001085) and the FENA (Grant 2009-NT-2048). J.B.K., S.S.L., and Y.L.L. also acknowledge funding by the Photovoltaics Program at ONR (N00014-11-10328) and an NSF-sponsored MRSEC through the Princeton Center for Complex Materials (DMR-0819860). Portions of this research were carried out at beamline 11-3 at SSRL, a national user facility operated by Stanford University on behalf of the U.S. Department of Energy, Office of Basic Energy Sciences, and at the Center for Functional Nano-materials, and beamline X-9 at BNL, which are supported by the U.S. Department of Energy, Office of Basic Energy Sciences, under Contract No. DE-AC02-98CH10886. We thank Chad Miller for assistance with data collection.

Supporting information for this article is available on the WWW under http://dx.doi.org/10.1002/anie.201203330.

of the two components and constructed photovoltaic devices from these mixtures. We found that the ratio of the two materials during spin-casting is vital for the efficiency of the device. The device in Figure 2 was made with a 1:2 molar ratio of 6-DBTTC:$PC_{70}BM$. For comparison, Figure S2 shows the

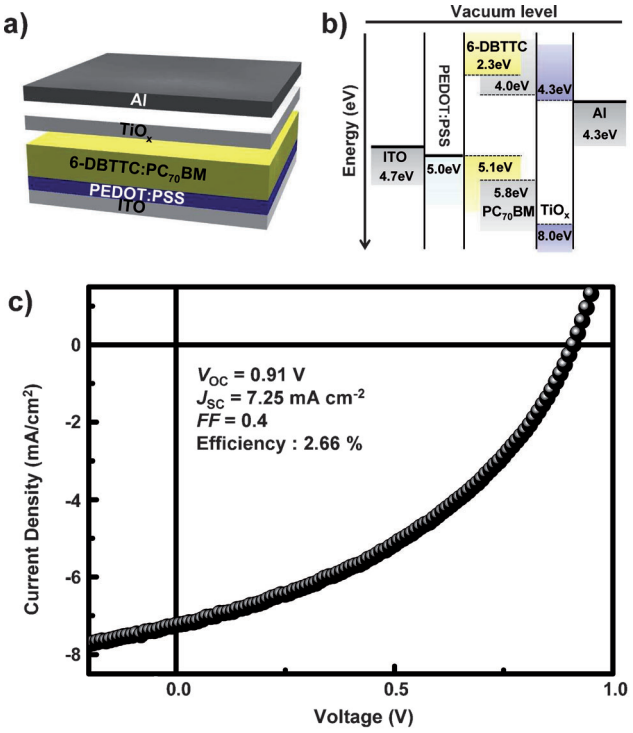

Figure 2. a) Schematic illustrations of the device architectures of the 6-DBTTC:$PC_{70}BM$ solar cell. b) Energy level diagram of the device components. c) Current density–voltage (*J–V*) characteristics of a representative device under light illumination.

current density–voltage (*J–V*) curves as a function of the molar ratio of 6-DBTTC and $PC_{60}BM$ in the solar cells.[12] $PC_{60}BM$ is another commonly used fullerene derivative in polythiophene:fullerene bulk heterojunction solar cells. We see that the PCE goes through a maximum at a ratio of 6-DBTTC:$PC_{60}BM$ = 1:2 and decreases by more than an order of magnitude when we deviate from that ratio.

Figure 2a shows the structure of an optimized photovoltaic device with 6-DBTTC and $PC_{70}BM$ as the active layer. The device consists of a spin-cast layer (≈60 nm thick) of a mixture of 6-DBTTC and $PC_{70}BM$ (in a ≈1:2 molar ratio) on top of a 30 nm thick PEDOT:PSS layer on an ITO-coated glass. The films were spun from a cosolvent of chlorobenzene (CB):dichlorobenzene (DCB) (1:1 w/w). An aluminum counter electrode was applied through thermal evaporation onto a titanium oxide (TiO_x) interlayer.[13–15] Figure 2b shows the energy levels of the individual components in the device. Current density–voltage (*J–V*) characteristics of each device were acquired using a Keithley 2635 source measurement unit under AM 1.5G 100 mW cm^{-2} illumination. The device achieves a V_{OC} of 0.91 ± 0.03 V, a short-circuit current density (J_{SC}) of 7.25 ± 0.2 mA cm^{-2}, and fill factor (*FF*) of 0.4, thus resulting in a PCE of 2.7 ± 0.1% across twelve devices (Figure 2c). Considering the absorption characteristics of 6-DBTTC, which is narrow and mainly absorbs in the UV range (≈370 nm, Figure S3), these solar cells are very efficient and show potential as transparent active layer to achieve totally transparent solar cells. The external quantum efficiency spectrum traces the 6-DBTTC:$PC_{70}BM$ UV-vis spectrum (Figure S3).

To understand the performance change with molar ratio of the organic semiconductor constituents, we created 6-DBTTC:$PC_{70}BM$ films on Si wafers (with 300 nm of thermal oxide) by drop-casting from a 0.1 wt% solution (solvent: *o*-xylene)[16] at various molar ratios of 6-DBTTC and $PC_{70}BM$ to increase crystallinity of blend films. We collected grazing-incidence wide-angle X-ray scattering (GIWAXS) patterns on these films (Figure 3). For the single component films, we

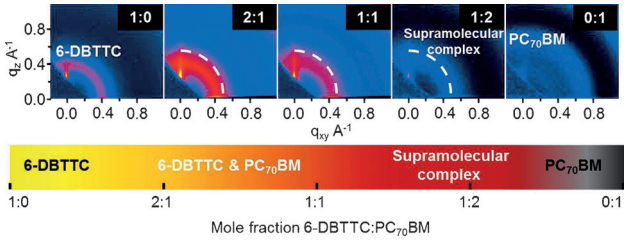

Figure 3. 2D GIWAXS patterns for 6-DBTTC:$PC_{70}BM$ films with different mixing ratios. Patterns from 2:1 and 1:1 films show reflections at q = 0.39 Å^{-1}, thus indicating the presence of 6-DBTTC crystals. A single reflection at q = 0.45 Å^{-1} was observed in films with a 1:2 molar ratio of 6-DBTTC:$PC_{70}BM$, presumably because of the formation of a supramolecular complex. The white dotted curve indicates the q value of the supramolecular complex.

observed a reflection at q = 0.39 Å^{-1} for 6-DBTTC and at 0.66 Å^{-1} for $PC_{70}BM$.[17] For diffraction patterns collected on films that are rich in 6-DBTTC (2:1 and 1:1 molar ratio of 6-DBTTC:$PC_{70}BM$), we saw the reflections of a distinct 6-DBTTC phase at q = 0.39 Å^{-1}. At lower 6-DBTTC concentrations similar to that used in the devices in Figure 2, we observed an interesting change in the diffraction patterns. These films exhibited a broad peak at q = 0.45 Å^{-1}. This reflection, albeit broad and weak, did not correspond to the reflection of pristine 6-DBTTC or $PC_{70}BM$. The conclusion we draw from this result is that the dominant contribution to this peak originates from a new phase that results from the assembly of the two components.[18]

We observed the same trends in the spin-cast films. Figure 4 shows the GIWAXS patterns of pure 6-DBTTC (at q = 0.39 Å^{-1}) and $PC_{70}BM$ (at q = 0.66 Å^{-1}). In contrast, the diffraction pattern of the film with a 1:2 molar ratio blend has a broad and diffuse reflection at 0.48 Å^{-1}. With even more $PC_{70}BM$ (1:4 molar ratio), this peak is much broader and weaker. The change in the *d*-spacing at certain mole fractions indicates the formation of a supramolecular complex in the film during the spin casting. One of the reasons for the formation of the supramolecular complex is that the doubly concave shape of 6-DBTTC is able to coordinate with the ball shape of $PC_{70}BM$ in the film to form a supramolecular complex. This supramolecular complex gives rise to the new

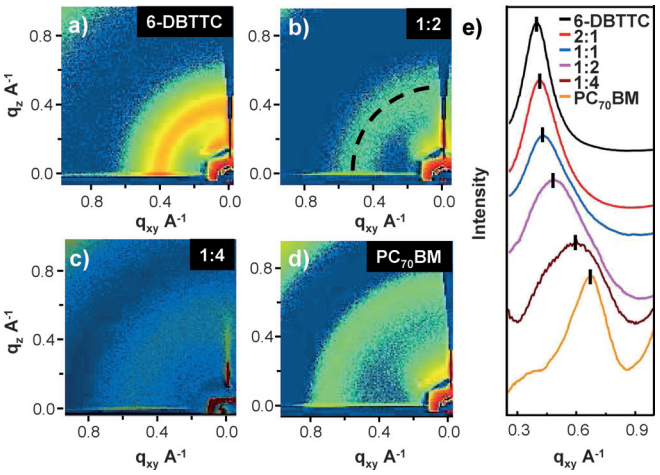

Figure 4. 2D GIWAXS patterns for spin-coated 6-DBTTC:$PC_{70}BM$ thin films at different molar ratios: a) 6-DBTTC, b) 1:2, c) 1:4, and d) $PC_{70}BM$. e) Intensity profile of GIWAXS data as a function of blend ratio. The reflection at $q = 0.48$ Å^{-1} in 1:2 molar ratio results from the supramolecular complex of 6-DBTTC and $PC_{70}BM$.

peak in the GIWAXS patterns and provides an efficient morphology in the solar cell.

To further investigate the supramolecular complex crystal in the 1:2 molar ratio film, we increased the crystallinity of the spin cast film using solvent annealing in a saturated *o*-xylene vapour chamber. Figure 5a shows a defocused bright field TEM image of the solvent annealed sample. The solvent

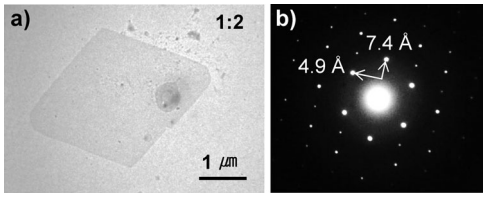

Figure 5. a) Bright-field TEM image shows a single crystal of the supramolecular complex (darker region). b) SAED pattern of single-crystal supramolecular complex.

annealed sample clearly shows non-uniform contrast resulting from the different phase contrast of new crystal domains in $PC_{70}BM$ medium. Single crystallinity of these new crystals is confirmed by selected area electron diffraction (SAED). The *d*-spacing of rectangular diffraction from the new crystalline state does not correspond to pristine 6-DBTTC or $PC_{70}BM$.[3,19] Thus the new crystal in the solvent annealed film forms between 6-DBTTC and $PC_{70}BM$ to give the supramolecular complex.

To support that the supramolecular complex is needed to provide the optimal device performance in our system, we applied standard methods that have been used in polymer bulk heterojunction (BHJ) solar cells by either thermal annealing after film deposition or incorporating additives into the solution prior to film deposition. Both of these methods have been shown to dramatically improve the efficiency of polymeric BHJ solar cells by inducing crystallization and phase separation between donor and acceptor.[20–22] We measured GIWAXS before and after these modifications. Upon heating of a film of 6-DBTTC:$PC_{70}BM$ in a molar ratio of 1:2 to 100 °C, at which 6-DBTTC starts to self-assemble,[3] the intensity of the reflection at $q = 0.48$ Å^{-1} dramatically decreases. If we continue heating the film to 150 °C for 5 min and then cool the film to room temperature, the fingerprint of the supramolecular complex at $q = 0.48$ Å^{-1} completely disappears in the GIWAXS pattern (see Figure S4a in the Supporting Information). The device performance also deteriorates dramatically after thermal annealing (Figure S4b). The optical microscope images in Figure S5 clearly show macrophase separation of 6-DBTTC in the film with the 1:2 ratio after thermal annealing at 150 °C for 5 min. Therefore, thermal annealing causes the pure 6-DBTTC phase to grow at the expense of the supramolecular complex and lowers the efficiency of the solar cell.

As another attempt to induce phase separation, we added processing additives, such as 1,8-octanedithiol and 1,8-diiodooctane, to the 6-DBTTC:$PC_{70}BM$ solution.[20,21] GIWAXS analysis on 6-DBTTC:$PC_{70}BM$ films incorporating these additives shows the presence of 6-DBTTC crystals, evidenced by a shoulder in the reflection at $q = 0.39$ Å^{-1} in the 1D plot (Figure S6). The formation of single-component crystals hinders the formation of the supramolecular complex structure, which in turn leads to poor device performance (Figure S7).

In previous studies, high PCE values in polymer[15,18–20] or small molecule[23–29] solar cells were usually obtained by inducing nanoscale phase separation between the electron donor and acceptor through thermal annealing or incorporation of processing additives into the active layer. In contrast, our studies show that for contorted molecular materials, the assembly between the two components is also an important parameter to control the photovoltaic properties. For the 6-DBTTC:$PC_{70}BM$ solar-cell system, we hypothesize that 6-DBTTC and $PC_{70}BM$ mix completely at the molecular level and the complex allows a more efficient charge separation. The GIWAXS images in Figure 3 and 4 support this argument because they show diffraction from $PC_{70}BM$ and the supramolecular complex, but not pure 6-DBTTC. This is consistent with the data for the 1:4 system (Figure 4c), in which the broad peak can be modeled as scattering from the supramolecular complex ($q = 0.48$ Å^{-1}) and pure $PC_{70}BM$ ($q = 0.66$ Å^{-1}). In our experimental conditions, weakly crystalline $PC_{70}BM$ is on the top surface of the film, thus allowing transfer of electrons to the cathode. We have further confirmed this hypothesis by fabricating inverted solar cell using ITO/TiO_x/6-DBTTC:$PC_{70}BM$/Au architecture. From the inverted solar cell, the weakly crystalline $PC_{70}BM$ molecules are in contact with the anode of the solar cell, thus making it impossible to obtain solar-cell-device properties. Thus, the supramolecular complex is located on the surface of the PEDOT:PSS layer, thus allowing transport of holes to the anode electrode.

In summary, this study shows that a supramolecular complex forms in the films blended with contorted 6-DBTTC:$PC_{70}BM$. These are the first fully solution-processed photovoltaic devices with this ball-and-socket motif. Forma-

tion of the supramolecular complex directly affects charge separation in the active layer, therefore leading to efficient small molecule BHJ organic solar cells. By forming structures composed of the donor and acceptor molecules in supramolecular heterojunction films, we achieve solar efficiencies of 2.7%. We believe that we can substantially improve this materials system by improving the light absorption of the molecules, but maintaining the ball and socket motif.

Received: April 30, 2012
Revised: May 29, 2012
Published online: July 13, 2012

Keywords: fullerenes · molecular electronics · organic semiconductors · organic solar cells · supramolecular chemistry

[1] N. J. Tremblay, A. A. Gorodetsky, M. P. Cox, T. Schiros, B. Kim, R. Steiner, Z. Bullard, A. Sattler, W. Y. So, Y. Itoh, M. F. Toney, H. Ogasawara, A. P. Ramirez, I. Kymissis, M. L. Steigerwald, C. Nuckolls, *ChemPhysChem* **2010**, *11*, 799 – 803.
[2] C. Y. Chiu, B. Kim, A. A. Gorodetsky, W. Sattler, S. J. Wei, A. Sattler, M. Steigerwald, C. Nuckolls, *Chem. Sci.* **2011**, *2*, 1480 – 1486.
[3] A. A. Gorodetsky, C. Y. Chiu, T. Schiros, M. Palma, M. Cox, Z. Jia, W. Sattler, I. Kymissis, M. Steigerwald, C. Nuckolls, *Angew. Chem.* **2010**, *122*, 8081 – 8084; *Angew. Chem. Int. Ed.* **2010**, *49*, 7909 – 7912.
[4] Z.-L. Zhong, A. Ikeda, S. Shinkai in *Calixarenes*, Kluwer Academic Publishers, Dordrecht, **2001**, pp. 476 – 495.
[5] P. E. Georghiou, L. N. Dawe, H. A. Tran, J. Strube, B. Neumann, H. G. Stammler, D. Kuck, *J. Org. Chem.* **2008**, *73*, 9040 – 9047.
[6] A. Sygula, F. R. Fronczek, R. Sygula, P. W. Rabideau, M. M. Olmstead, *J. Am. Chem. Soc.* **2007**, *129*, 3842 – 3843.
[7] L. C. Palmer, S. I. Stupp, *Acc. Chem. Res.* **2008**, *41*, 1674 – 1684.
[8] G. Bottari, G. de La Torre, D. M. Guldi, T. Torres, *Chem. Rev.* **2010**, *110*, 6768 – 6816.
[9] F. Silvestri, I. Lopez-Duarte, W. Seitz, L. Beverina, M. V. Martinez-Diaz, T. J. Marks, D. M. Guldi, G. A. Pagani, T. Torres, *Chem. Commun.* **2009**, 4500 – 4502.
[10] C. L. Wang, W. B. Zhang, R. M. Van Horn, Y. F. Tu, X. Gong, S. Z. D. Cheng, Y. M. Sun, M. H. Tong, J. Seo, B. B. Y. Hsu, A. J. Heeger, *Adv. Mater.* **2011**, *23*, 2951 – 2956.
[11] J. Wang, D. L. Wang, E. K. Miller, D. Moses, G. C. Bazan, A. J. Heeger, *Macromolecules* **2000**, *33*, 5153 – 5158.
[12] For higher throughput in these screening measurements, we did not include the titania layer, and we substituted $PC_{70}BM$ with phenyl-C_{60}-butyric acid methyl ester ($PC_{60}BM$). The trend is the same, with or without these changes.
[13] J. Y. Kim, S. H. Kim, H. H. Lee, K. Lee, W. L. Ma, X. Gong, A. J. Heeger, *Adv. Mater.* **2006**, *18*, 572 – 576.
[14] C. S. Kim, S. S. Lee, E. D. Gomez, J. B. Kim, Y. L. Loo, *Appl. Phys. Lett.* **2009**, *94*, 113302.
[15] C. J. Brabec, A. Cravino, D. Meissner, N. S. Sariciftci, T. Fromherz, M. T. Rispens, L. Sanchez, J. C. Hummelen, *Adv. Funct. Mater.* **2001**, *11*, 374 – 380.
[16] The 2D GIWAXS images are independent of solvents (CB, mixture of CB and DCB, and *o*-xylene).
[17] E. Verploegen, R. Mondal, C. J. Bettinger, S. Sok, M. F. Toney, Z. A. Bao, *Adv. Funct. Mater.* **2010**, *20*, 3519 – 3529.
[18] A. C. Mayer, M. F. Toney, S. R. Scully, J. Rivnay, C. J. Brabec, M. Scharber, M. Koppe, M. Heeney, I. McCulloch, M. D. McGehee, *Adv. Funct. Mater.* **2009**, *19*, 1173 – 1179.
[19] L. D. Zheng, Y. C. Han, *J. Phys. Chem. B* **2012**, *116*, 1598 – 1604.
[20] J. K. Lee, W. L. Ma, C. J. Brabec, J. Yuen, J. S. Moon, J. Y. Kim, K. Lee, G. C. Bazan, A. J. Heeger, *J. Am. Chem. Soc.* **2008**, *130*, 3619 – 3623.
[21] Y. Yao, J. H. Hou, Z. Xu, G. Li, Y. Yang, *Adv. Funct. Mater.* **2008**, *18*, 1783 – 1789.
[22] M. T. Dang, L. Hirsch, G. Wantz, *Adv. Mater.* **2011**, *23*, 3597 – 3602.
[23] M. T. Lloyd, J. E. Anthony, G. G. Malliaras, *Mater. Today* **2007**, *10*, 34 – 41.
[24] C. Q. Ma, M. Fonrodona, M. C. Schikora, M. M. Wienk, R. A. J. Janssen, P. Bauerle, *Adv. Funct. Mater.* **2008**, *18*, 3323 – 3331.
[25] B. Walker, A. B. Tomayo, X. D. Dang, P. Zalar, J. H. Seo, A. Garcia, M. Tantiwiwat, T. Q. Nguyen, *Adv. Funct. Mater.* **2009**, *19*, 3063 – 3069.
[26] W. W. H. Wong, T. B. Singh, D. Vak, W. Pisula, C. Yan, X. L. Feng, E. L. Williams, K. L. Chan, Q. H. Mao, D. J. Jones, C. Q. Ma, K. Mullen, P. Bauerle, A. B. Holmes, *Adv. Funct. Mater.* **2010**, *20*, 927 – 938.
[27] B. Walker, C. Kim, T. Q. Nguyen, *Chem. Mater.* **2011**, *23*, 470 – 482.
[28] W. W. H. Wong, C. Q. Ma, W. Pisula, C. Yan, X. L. Feng, D. J. Jones, K. Mullen, R. A. J. Janssen, P. Bauerle, A. B. Holmes, *Chem. Mater.* **2010**, *22*, 457 – 466.
[29] N. M. Kronenberg, M. Deppisch, F. Wurthner, H. W. A. Lademann, K. Deing, K. Meerholz, *Chem. Commun.* **2008**, 6489 – 6491.

